

Supporting Information (SI)

Thickening of liquids using copolymer grafted nanoparticles

Prama Adhya¹, Sachin M. B. Gautham^{2,4}, Tarak K Patra^{2,4*}, Manish Kaushal^{1*}, Titash Mondal^{3*}

¹Department of Chemical Engineering, Indian Institute of Technology Kharagpur, Kharagpur-721302, India

³Rubber Technology Center, Indian Institute of Technology Kharagpur, Kharagpur-721302, India

²Department of Chemical Engineering, Indian Institute of Technology Madras, Chennai-600036, India

⁴Center for Atomistic Modeling and Materials Design, Indian Institute of Technology Madras, Chennai-600036, India

*Corresponding Authors.

E-mails: titash@rtc.iitkgp.ac.in (TM), mkaushal@che.iitkgp.ac.in (MK), tpatra@smail.iitm.ac.in (TKP)

1. Materials:

Silica nanoparticles, with a specific surface area ranging from 175 m²/g to 225 m²/g, was provided by Degussa. Jeffamine M 2070, a polyetheramine, was generously supplied by Huntsman Corporation, India. Isocyanate-terminated alkoxy silane, Silquest A-Link 35, was received from Momentive Performance Materials, India. Toluene, with a purity of 99.5%, was procured from Emparta and used as a solvent. All materials were used without further purification.

2. Synthesis of silane capped amine terminated copolymer and its grafting on the surface of silica nanoparticles:

Polyetheramine (Jeffamine M 2070) was placed in a round-bottom flask and heated at a constant temperature of 80°C. 3-Isocyanatopropyl Trimethoxysilane was then added to the solution and stirred for 24 hours, maintaining a 1:1 molar ratio of the two compounds. The resulting polymer was grafted onto the surface of silica nanoparticles. Before the grafting process, the silica nanoparticles (Si) was heated for 24 hours to remove any moisture. The nanoparticles was then dispersed in a mixture of toluene and water and sonicated for 30 minutes to break up any agglomerates. The synthesized polymer was added dropwise to the silica dispersion and stirred at room temperature for 24 hours. The Grafted nanoparticles (GNP) was collected by centrifugation at 1000 rpm and washed multiple times with toluene. It was then

dried in an oven at 75-80°C for 24 hours and collected in powder form. The grafting was confirmed using Fourier Transform Infrared (FTIR) analysis.

3. Analytical Characterization:

Fourier Transform Infrared Spectroscopy (FTIR) was performed using a Spectrum 100 model from Perkin Elmer, USA. Thermogravimetric Analysis (TGA) was carried out using a TGA 50 model from Shimadzu, Japan. Samples were heated from 25°C to 800°C at a rate of 10°C per minute under a 40 mL/min air flow. Differential scanning calorimetry (DSC) analysis was conducted using a NETZSCH DSC 200 F3 instrument -TA Instruments, Germany. Static Light Scattering (SLS) measurements were carried out using a system from Photocor Ltd., equipped with a Ga-As diode laser operating at a wavelength of 658.3 nm and an output power of 35 mW. Scattered light intensity fluctuations were recorded at angles ranging from 30° to 110°.

3.1. FTIR Analysis:

FT-IR confirms the synthesis of the co-polymer from the monomers as well as the grafting of the co-polymer on the surface of the silica nanoparticles. FTIR analysis of the synthesised product confirms that silane capped polymer has been formed as explained below in **figure S1a**.

The peaks of pure Polyetheramine are exhibited at 846 cm^{-1} for N-H- stretching, 2986 cm^{-1} -C-H- stretching and 1378 cm^{-1} for -CH₂- stretching.¹ The monomer 3-Isocyanatopropyl Trimethoxysilane exhibited peaks at 1097 cm^{-1} for -C-N- stretching, 2986 cm^{-1} for -C-H- stretching. The co-polymer has a urea linkage thus, a new peak was formed at 1640 cm^{-1} and 1570 cm^{-1} .² The peaks present in A-link 35 and Jeffamine are present in the synthesised co-polymer. Thus, the synthesis of the polymer formed can be justified from the above shown FTIR data.³ Further, the comparison of the silica nanoparticle and the polymer GNP at different ratios (1:0.5, 1:1, 1:2 and 1:3) are shown in the FTIR plot below. As shown in **Figure S1b**, the GNP show peaks at 2986 cm^{-1} , -C-H- stretching and 1378 cm^{-1} for -CH₂-CH₂ stretching, 2986 cm^{-1} for -C-H- stretching, due to the formation of the urea linkage new peak was formed at 1640 cm^{-1} and 1570 cm^{-1} . The observation of the urea linkage substantiated the successful formation of the silane terminated polyetheramine. The reaction between the methoxy group of the polymer and the silanol group of the silica was observed and was substantiated by the disappearance of the methoxy group and formation of Si-O-Si linkage at 1127 cm^{-1} .⁴

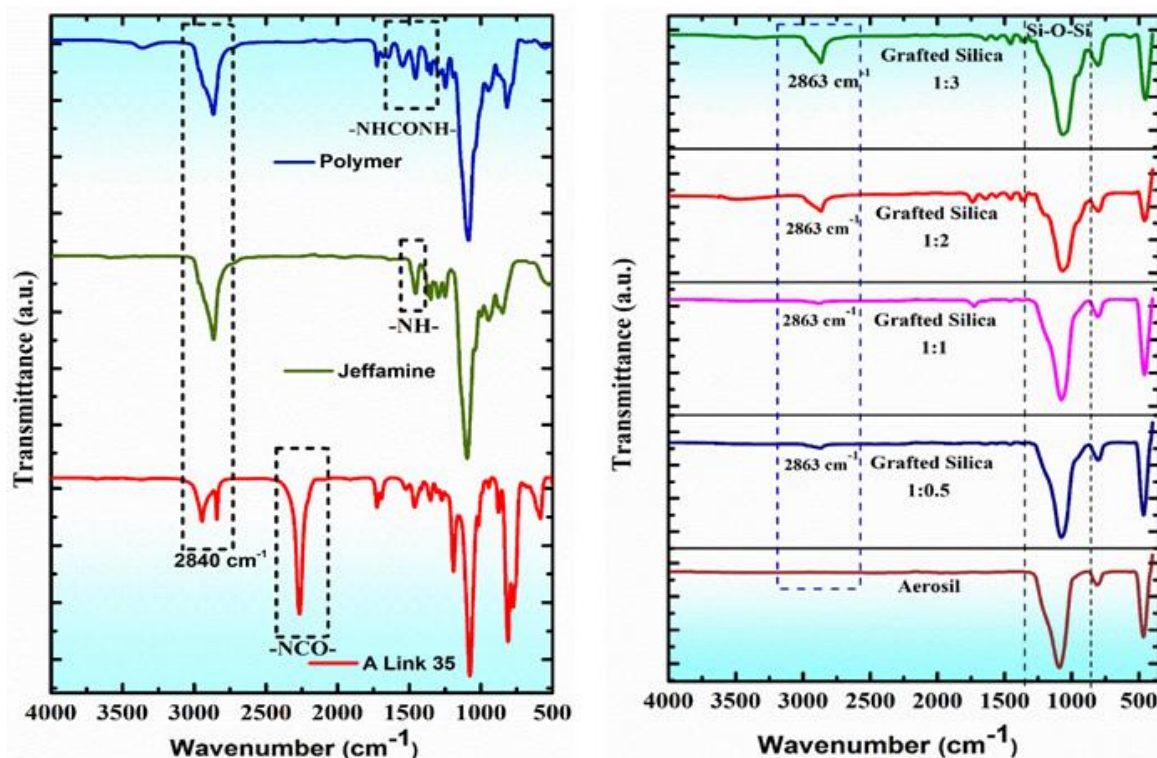


Figure S1a: FTIR spectra for Jeffamine, Silquest A Link- 35 and silane capped amine terminated co-polymer respectively measured in the ATR mode. **Figure S1b:** FTIR spectra for the comparison of bare silica and the polymer GNP (grafted at different ratios of 1:0.5, 1:1, 1:2, 1:3) of the polymer grafted silica sample.

3.2. Thermogravimetric analysis:

Thermogravimetric Analysis (TGA)⁵ of the samples was carried out from 25° to 800°C at a ramp of 10°C rise per minute under a 40mL/min air flow per minute to check the weight loss.⁶ The impact of surface modification was studied using the TGA where the grafting density was also calculated from the weight loss observed as shown in **figure S2a**.⁷ The GNP with ratio 1:0.5, 1:1, 1:1.5, 1:1.5, 1:2 and 1:3 (where the ratio of the polymer has been varied) demonstrated a weight loss of 28.77%, 33.14%, 40.13%, 53.25% and 58.95% respectively.⁸ The grafting density of the silica nanoparticles as well as GNP can be found out using the TGA curve.⁴ The weight loss percentage is used here for the calculation of the grafting density, using formula,

$$\text{Grafting Density} = \frac{(A-B)}{M_w * S_p} N_A \quad (1)$$

where, A = (% weight loss of modified silica) / (100 – % weight loss of modified silica),
 B = (% weight loss of unmodified silica) / (100- % weight loss of unmodified silica),
 N_A = Avogadro's number, M_w = molecular weight and S_p = Surface area of the nanoparticles.

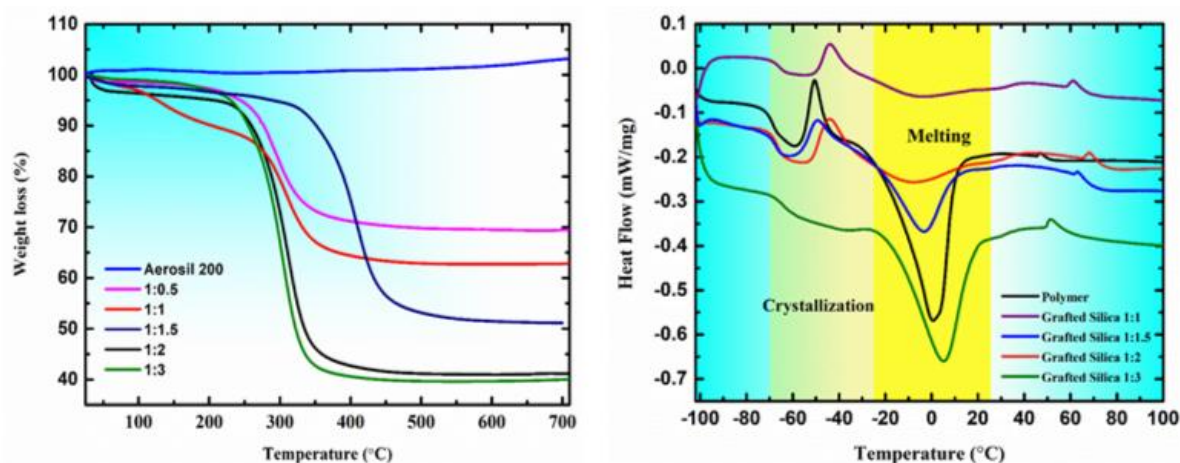


Figure S2a: TGA analysis of Polymer Grafted silica at different ratios are reported in the graph. **Figure S2b:** DSC curve showing comparison among polymer and polymer GNP with ratio 1:1, 1:1.5, 1:2 and 1:3.

From **figure S2a**, we can see that the silica particle demonstrated negligible weight loss. Hence, the factor B in the above equation can be neglected. Utilizing the molecular weight of the polymer, 2116 g/mol (determined experimentally), and the surface area of silica, 2×10^{20} nm²/g, in equation (1), the grafting density obtained for modified silica for various grafting ratios (1:0.5, 1:1, 1:1.5, 1:2 and 1:3) are reported in table-S1.⁹ When the tether density is calculated to be greater than 5 it can be confirmed as a polymer brush structure.¹⁰ For the GNP the tether density is seen to increase respectively with the increase in the grafting ratios. The highest tether density of 11.303 in our case is found for 1:3 GNP¹¹ Thus, we can confirm the polymer mushroom to brush transition by monitoring the reduced tether density. The data is further given in table S1 below, where the variation of grafting density with the increase in polymer ratio is shown.

Grafting ratio	Weight loss (%)	Grafting density Σ (chains/nm ²)	Tether Density ($\Sigma\pi Rg^2$)
1:0.5	28.771	0.5747	3.188
1:1	33.142	0.705	3.91
1:1.5	40.81	0.982	4.1
1:2	53.25	1.622	9.014
1:3	58.95	2.035	11.303

Table S1: Variation of grafting density with ratio of polymer grafting on silica nanoparticles

3.3. Differential Scanning Calorimetry (DSC):

Differential Scanning Calorimetry (DSC)¹² was done for the GNP at constant rate of heating 10°/min under nitrogen flow at 40mL/min. The melting and the crystallization rates was checked from this.⁵ The differential scanning calorimetry was used to determine the thermal transition of the polymer and GNP as shown in the **figure S2b** above. The glass transition temperature of polymer was found at -66.5°C. An increase in the transition temperature was observed in the polymer grafted on the silica nanoparticle due to the anchoring of the polymer chain in the neighbourhood of the nanoparticle.¹³ As the mobility of the chain is arrested, more energy is required to pass from the glassy regime to the rubbery regime. The entropy of the polymer chain gets reduced on the interface and acts like an immobilized layer on the particle. A temperature broadening of the transition was also found in these polymer grafted silica samples.¹⁴

Similarly, the shift in the crystallization temperature was observed in the GNP with different ratios as compared to neat polymer. The grafted polymer chains help in the crystallization of the polymer due to free space among the polymer chain helping to orient themselves.¹⁵ This phenomenon was observed in an evident manner in samples with grafting ratio 1:1 followed by 1:1.5 and 1:2. Though in case of GNP with ratio 1:3 with the highest graft density sample, the polymer chain is crowded and behaves like a secondary round bodies. Hence the crystallization temperature of this sample was not found in the DSC curve. With the increase in the grafting density the crystallinity did not occur. The crystallization of the polymer takes place at -50°C whereas in case of GNP the crystallization temperature shifts to -40°C in case of 1:2 grafting and -45°C in case of 1:1 GNP. The melting point of the polymer is at 0°C which helps in determining the crystallinity is similar to the melting point of GNP which is -10°C. It forms the highest crystalline domain among which can be confirmed the largest area under the crystalline curve. In the case of GNP, the maximum crystalline domain was found in GNP with ratio 1:3 where the grafting density is highest followed by GNP with ratio 1:2 and 1:1. Thus we can conclude that the crystalline domain increases by enhancing the grafting density.¹⁶

3.4. Static Light Scattering:

SLS was conducted at angles ranging from 30° to 110°. The partial Zimm plot was analysed, to calculate the radius of gyration of the polymer sample was calculated. The polymer was diluted to a molar solution with a tenfold dilution. Analysis was carried out with laser light at angles from 10° to 110°. Using the data, a partial Zimm plot was constructed, revealing a radius

of gyration of 1.33×10^{-9} meters, as shown in **figure S3a** below. This radius of gyration was then used to calculate the reduced tether density, confirming the structure to be a polymer brush **figure S3b**.

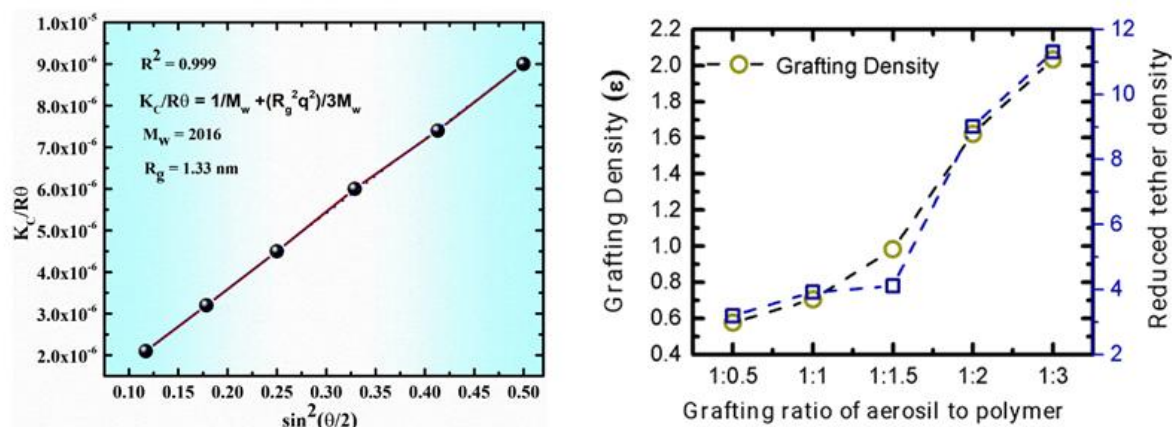


Figure S3a: The radius of gyration obtained from the partial zimm plot obtained from the static light scattering experiment. **Figure 3b:** Grafting density and reduced tether density of various polymer brush modified GNP particles as a function of various grafting ratio of silica to polymer.

4. Gel permeation chromatography (GPC)

The GPC trace data of silane terminated polyether is shown in figure S4.

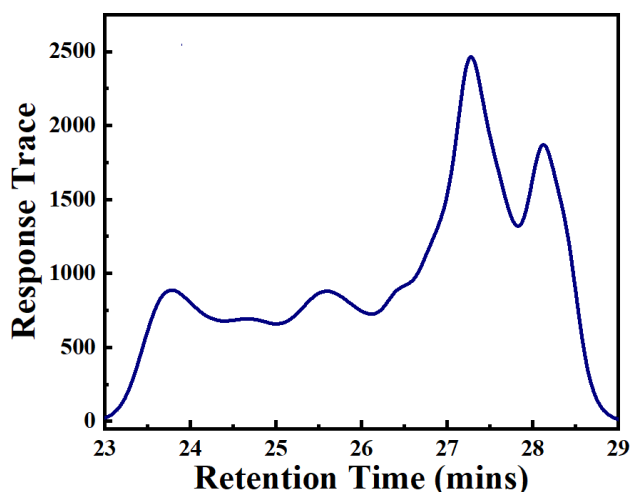


Figure S4: GPC trace data of silane terminated polyetheramine.

The molecular weight of the synthesized polymer was calculated using the software available with the instrument. Narrowly dispersed polystyrene standards were used for calibration purposes. The polymer solution was passed through three PLgel columns, with a guard column placed before them. A refractive index detector was used to record the signal.

5. Rheological Characterization

The MCR-302 rheometer (@Anton-paar) was used for rheological characterization of all dispersions. For viscosity measurement, we have used the methodology proposed by Cagny et al.¹⁷, wherein oscillatory strain amplitude sweep data was used to generate flow curves in terms of stress as a function of shear rate. More specifically, we have also conducted the strain amplitude sweep test, $\gamma = \gamma_0 \sin \omega t$ (where γ_0 and ω are the strain amplitude and oscillation frequency, respectively), to obtain stress amplitude (σ_0) as a function of shear rate ($\dot{\gamma} = \gamma_0 \omega$). This data has been further used to calculate shear rate dependent viscosity ($\eta = \sigma_0 / \dot{\gamma}$). Finally, we have calculated the normalized viscosity $\eta_r = \eta / \eta_0$, where η_0 is the viscosity of pure polymer matrix.

6. Model and Simulations

Polymer chains (both free chains and graft chains) are represented as the Kremer and Grest¹⁸ bead-spring model. In this model, two adjacent monomers of a polymer chain are connected by the Finite Extensible Nonlinear Elastic (FENE) potential of the form $E_{bond}(r_{ij}) = -0.5kR_0^2 \ln \left[1 - \left(\frac{r_{ij}}{R_0} \right)^2 \right] + 4\epsilon \left[\left(\frac{\sigma}{r} \right)^{12} - \left(\frac{\sigma}{r} \right)^6 \right] + \epsilon$. The second term in $E_{bond}(r_{ij})$ is truncated at $r = 2^{1/6}\sigma$. The maximum extent of the bond is $R_0 = 1.5\sigma$, and $k = 30\epsilon$. Here, ϵ and σ are the cohesive energy and size of a monomer. The non-bonded monomers interact via the Lennard-Jones (LJ) potential of the form $V(r) = 4\epsilon \left[\left(\frac{\sigma}{r} \right)^{12} - \left(\frac{\sigma}{r} \right)^6 \right]$, truncated and shifted to zero at a cut-off distance $r_c = 2.5\sigma$. The interaction between free chains and graft chains are also modelled via the LJ interaction. The cut-off distance for A-type moiety and free chain monomer pair is $r_c = 2.5\sigma$. The cut-off distance for B-type moiety and free chain monomer pair is $r_c = 1.122\sigma$. The NP-NP interaction and NP-monomer (both free chains and graft chains) interaction are modelled by the shifted LJ potential of the form $V_s(r) = 4\epsilon \left[\left(\frac{\sigma}{r-\Delta} \right)^{12} - \left(\frac{\sigma}{r-\Delta} \right)^6 \right]$ with a cut-off distance of $2^{1/6}\sigma + \Delta$. We choose $\Delta=2\sigma$ for NP-NP interaction, and $\Delta=1\sigma$ for NP-monomer interaction. The graft chains are of length 10. A NP and the grafted monomers of all the grafted chains on it move as a rigid body during an MD simulation.¹⁹ The polymer-NP interaction is attractive to model the bare NP case, which is implemented by choose a cut-off distance of $2.5\sigma + \Delta$ for the $V_s(r)$. We conduct CGMD simulations for NP loading $\phi=0.02$ and grafting density $\Sigma = 0.9 \sigma^{-2}$. The simulation box consists of 8 NPs, 2051 free chains and 13 grafted chains. We use the velocity-verlet algorithm

with a time-step of 0.005τ to integrate the equations of motions. Here, $\tau = \sigma\sqrt{m/\epsilon}$ is the unit of time, and m is the mass of a monomer. The Newton's equation of motion of all the particles are integrated in a canonical ensemble (NPT) at a reduced temperature $T^* = k_B T/\epsilon = 1.0$ and reduced pressure $P^* = P\sigma^3/\epsilon = 1.0$. The k_B is the Boltzmann constant. All the systems are equilibrated for 10^8 MD steps, followed by a production run for 10^7 MD steps. The NP-NP pair correlations functions are calculated using the production trajectories.

Furthermore, the NPT equilibrated structures are used for non-equilibrium molecular dynamics (NEMD) simulations for shear-dependent viscosity calculations. In the NEMD simulations, the SLLOD equation of motion²⁰ of all the particles are integrated using the velocity-Verlet algorithm in a canonical ensemble (NVT). In these simulations, a shear is applied to the simulation box in the xy -plane with a constant rate. We perform an initial 10^7 MD steps to achieve a steady state, followed by a production run of an additional 10^7 MD steps. We calculate the viscosity from the production trajectory of the system. The shear stress μ_{xy} is computed as the average of each particle stress given by $\mu_{xy} = \frac{1}{2Nv} \sum_{i=1}^N \sum_{i \neq j} r_{xij} F_{yij}$ where, $v = L^3/N$ is the average bead volume, L is the box length, and r_{xij} and F_{yij} are the x-component of the separation between the i^{th} and j^{th} bead and the y-component of their force. The shear viscosity (η) is calculated as $\eta = -\mu_{xy}/\dot{\gamma}$. We vary the shear rate from $\dot{\gamma} = 10^{-5}$ to $\dot{\gamma} = 10^0$.

References:

- (1) Ren, G.; Zheng, X.; Gu, H.; Di, W.; Wang, Z.; Guo, Y.; Xu, Z.; Sun, D. Temperature and CO₂ Dual-Responsive Pickering Emulsions Using Jeffamine M2005-Modified Cellulose Nanocrystals. **2019**. <https://doi.org/10.1021/acs.langmuir.9b02497>.
- (2) Jiang, L.; Ctor Bagá, H.; Kamra, T.; Zhou, T.; Ye, L. Nanohybrid Polymer Brushes on Silica for Bioseparation †. *J Mater Chem B* **2016**, *4*, 3247. <https://doi.org/10.1039/c6tb00241b>.
- (3) Alotaibi, K. M. Mesoporous Silica Nanoparticles Modified with Stimuli-Responsive Polymer Brush as an Efficient Adsorbent for Chlorophenoxy Herbicides Removal from Contaminated Water. **2021**. <https://doi.org/10.1080/03067319.2021.1907362>.
- (4) Mondal, T.; Ashkar, R.; Butler, P.; Bhowmick, A. K.; Krishnamoorti, R. Graphene Nanocomposites with High Molecular Weight Poly(ϵ -Caprolactone) Grafts: Controlled Synthesis and Accelerated Crystallization. *ACS Macro Lett.* **2016**, *5* (3), 278–282. <https://doi.org/10.1021/acsmacrolett.5b00930>.
- (5) Watson, E. S.; O'Neill, M. J.; Justin, J.; Brenner, N. A Differential Scanning Calorimeter for Quantitative Differential Thermal Analysis. *Anal. Chem.* **1964**, *36* (7), 1233–1238. <https://doi.org/10.1021/ac60213a019>.
- (6) Kunc, F.; Balhara, V.; Sun, Y.; Daroszewska, M.; Jakubek, Z. J.; Hill, M.; Brinkmann, A.; Johnston, L. J. Quantification of Surface Functional Groups on Silica Nanoparticles:

- Comparison of Thermogravimetric Analysis and Quantitative NMR †. *Cite This Anal.* **2019**, *144*, 5589. <https://doi.org/10.1039/c9an01080g>.
- (7) Morinaga, T.; Honma, S.; Ishizuka, T.; Kamijo, T.; Sato, T.; Tsujii, Y. Synthesis of Monodisperse Silica Particles Grafted with Concentrated Ionic Liquid-Type Polymer Brushes by Surface-Initiated Atom Transfer Radical Polymerization for Use as a Solid State Polymer Electrolyte. <https://doi.org/10.3390/polym8040146>.
 - (8) Le-Masurier, S. P.; Gody, G.; Perrier, S.; Granville, A. M. One-Pot Polymer Brush Synthesis via Simultaneous Isocyanate Coupling Chemistry and “Grafting from” RAFT Polymerization †. **2014**. <https://doi.org/10.1039/c4py00025k>.
 - (9) Matsuda, Y.; Kobayashi, M.; Annaka, M.; Ishihara, K.; Takahara, A. Dimensions of a Free Linear Polymer and Polymer Immobilized on Silica Nanoparticles of a Zwitterionic Polymer in Aqueous Solutions with Various Ionic Strengths. <https://doi.org/10.1021/la8005647>.
 - (10) Jiang, L.; Ctor Bagá, H.; Kamra, T.; Zhou, T.; Ye, L. Nanohybrid Polymer Brushes on Silica for Bioseparation †. *J Mater Chem B* **2016**, *4*, 3247. <https://doi.org/10.1039/c6tb00241b>.
 - (11) Liu, G.; Cai, M.; Zhou, F.; Liu, W. Charged Polymer Brushes-Grafted Hollow Silica Nanoparticles as a Novel Promising Material for Simultaneous Joint Lubrication and Treatment. **2014**. <https://doi.org/10.1021/jp500074g>.
 - (12) Hesketh, T. R.; Van Bogart, J. W. C.; Cooper, S. L. *Differential Scanning Calorimetry Analysis of Morphological Changes in Segmented Elastomers*.
 - (13) He, L.; Huang, J.; Chen, Y.; Xu, X.; Liu, L. Inclusion Interaction of Highly Densely PEO Grafted Polymer Brush and R-Cyclodextrin. **2005**. <https://doi.org/10.1021/ma0475333>.
 - (14) Savin, D. A.; Pyun, J.; Patterson, G. D.; Kowalewski, T. Synthesis and Characterization of Silica-Graft-Polystyrene Hybrid Nanoparticles: Effect of Constraint on the Glass-Transition Temperature of Spherical Polymer Brushes*. **2002**. <https://doi.org/10.1002/polb.10329>.
 - (15) Sakib, N.; Koh, Y. P.; Huang, Y.; Mongcopa, K. I. S.; Le, A. N.; Benicewicz, B. C.; Krishnamoorti, R.; Simon, S. L. Thermal and Rheological Analysis of Polystyrene-Grafted Silica Nanocomposites. *Macromolecules* **2020**, *53*, 2123–2135. <https://doi.org/10.1021/acs.macromol.9b02127>.
 - (16) Jiang, X.; Zhong, G.; Horton, J. M.; Jin, N.; Zhu, L.; Zhao, B. Evolution of Phase Morphology of Mixed Poly(Tert-Butyl Acrylate)/ Polystyrene Brushes Grafted on Silica Particles with the Change of Chain Length Disparity. *Macromolecules* **2010**, *43*, 5387–5395. <https://doi.org/10.1021/ma100716n>.
 - (17) de Cagny, H.; Fazilati, M.; Habibi, M.; Denn, M. M.; Bonn, D. The Yield Normal Stress. *J. Rheol.* **2019**, *63* (2), 285–290. <https://doi.org/10.1122/1.5063796>.
 - (18) Kremer, K.; Grest, G. S. Dynamics of Entangled Linear Polymer Melts: A Molecular-Dynamics Simulation. *J. Chem. Phys.* **1990**, *92* (8), 5057–5086. <https://doi.org/10.1063/1.458541>.
 - (19) Miller, T. F.; Eleftheriou, M.; Pattnaik, P.; Ndirango, A.; Newns, D.; Martyna, G. J. Symplectic Quaternion Scheme for Biophysical Molecular Dynamics. *J. Chem. Phys.* **2002**, *116* (20), 8649–8659. <https://doi.org/10.1063/1.1473654>.
 - (20) Daivis, P. J.; Todd, B. D. A Simple, Direct Derivation and Proof of the Validity of the SLLD Equations of Motion for Generalized Homogeneous Flows. *J. Chem. Phys.* **2006**, *124* (19), 194103. <https://doi.org/10.1063/1.2192775>.

